MATLAB SIMULATION OF SINGLE-INPUT MULTIPLE-OUTPUT DC-DC CONVERTER

Rakesh Sonkusare[1] Pranali Bante[2] Sarita Manjarkhede[3]
Vikrant Bais[4] Shashikant Shinde[5]
DEPARTMENT OF ELECTRICAL ENGINEERING (ELECTRONICS & POWER)
KARMAVEER DADASAHEB KANNAMWAR COLLEGE OF ENGINEERING, NAGPUR
rakeshssonkusare@gmail.com[1] panub.2003@gmail.com[2]

***Abstract*—The aim of this study is to develop a high-efficiency single-input multiple-output (SIMO) dc–dc converter. The proposed converter can boost the voltage of a low-voltage input power source to a controllable high-voltage dc bus and middle-voltage output terminals. The high-voltage dc bus can take as the main power for a high-voltage dc load or the front terminal of a dc–ac inverter. Moreover, middle-voltage output terminals can supply powers for individual middle-voltage dc loads or for charging auxiliary power sources (e.g., battery modules). In this study, a coupled-inductorbased dc–dc converter scheme utilizes only one power switch with the properties of voltage clamping and soft switching, and the corresponding device specifications are adequately designed. As a result, the objectives of high-efficiency power conversion, high stepup ratio, and various output voltages with different levels can be obtained. Some experimental results via a kilowatt-level prototype are given to verify the effectiveness of the proposed SIMO dc–dc converter in practical applications.**

***Index Terms*—Coupled inductor, high-efficiency power conversion, single-input multiple-output (SIMO) converter, soft switchin and voltage clamping.**

I. INTRODUCTION

In recent years the demand of energy is growing, rising the public awareness for environment. To protect the earth from global warming, created demand for the development of clean energy without pollution, have resulted in much of the research work focused on clean energies, such as fuel cell (FC), photovoltaic, and wind energy, etc. Due to the electric characteristics of clean energy, the generated power is critically affected by the climate or has slow transient responses, and the output voltage is easily influenced by load variations. Besides, other auxiliary components,e.g., storage elements, control boards, etc., are usually required to ensure the proper operation of clean energy. For example, an FC-generation system is one of the most efficient and effective solutions to the environmental pollution problem. In addition to the FC stack itself, some other auxiliary components, such as the balance of plant (BOP) including an electronic control board, an air compressor, and a cooling fan, are required for the normal work of an FC generation system. In other words, the generated power of the FC stack also should satisfy the power demand for the BOP. Thus, various voltage levels should be required in the power converter of an FC generation system. In general, various single-input single-output dc–dc converters with different voltage gains are combined to satisfy the requerment of various voltage levels, so that its system control is more complicated and the corresponding cost is more expensive. The motivation of this project is to designe a SIMO converter for increasing the conversion efficiency and voltage gain, redusing the control complexity and saving the manufacturing cost. Single Input Multiple Output (SIMO) converters are widely used in industrial applications. Converters having single input source and generating more than one isolated or non-isolated output voltage are called Single Input Multiple Output (SIMO) converters. Small size and high efficiency are attractive features of any converter.

Patra *et al* presented a SIMO dc–dc converter capable of generating buck, boost, and inverted outputs simultaneously. However, over three switches for one output were required. This scheme is only suitable for the low output voltage and power application, and its power conversion is degenerated due to the operation of hard switching. Nami*et al.* proposed a new dc–dc multi-output boost converter, which can share its total output

between different series of output voltages for low- and high-power applications. Unfortunately, over two switches for one output were required, and its control scheme was complicated. Besides, the corresponding output power cannot supply for individual loads independently. Chen *et al.* investigated a multiple-output dc–dc converter with shared zero-currentswitching (ZCS) lagging leg. Although this converter with the soft-switching property can reduce the switching losses, this combination scheme with three full-bridge converters is more complicated, so that the objective of high-efficiency power conversion is difficult to achieve, and its cost is inevitably increased. This study presents a newly designed SIMO converter with a coupled inductor.

The proposed converter uses one power switch to achieve the objectives of high-efficiency power conversion, high step-up ratio, and different output voltage levels. In the proposed SIMO converter, the techniques of soft switching and voltage clamping are adopted to reduce the switching and conduction losses via the utilization of a low-voltage-rated power switch with a small *R*DS(on) . Because the slew rate of the current change in the coupled inductor can be restricted by the leakage inductor, the current transition time enables the power switch to turn ON with the ZCS property easily, and the effect of the leakage inductor can alleviate the losses caused by the reverse-recovery current. Additionally, the problems of the stray inductance energy and reverse-recovery currents within diodes in the conventional boost converter also can be solved, so that the high-efficiency power conversion can be achieved. The voltages of middle-voltage output terminals can be appropriately adjusted by the design of auxiliary inductors; the output voltage of the high-voltage dc bus can be stably controlled by a simple pulse width modulation (PWM) control.

II. Converter Design and Analyses

The block diagram of praposed high efficiency single input multiple output converter to generate two different voltage levels from single input power source is shown in fig.1.In this, the dc voltage from the source is fed into dc-dc converter, it could boost the input voltage and the boosted voltage is connected to various loads. This converter has a multiple output voltages. That is low voltage and high voltage output terminals. This converter is controlled by a PWM controller.

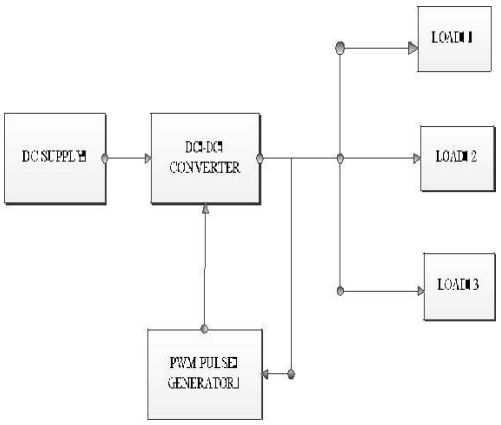

Fig. 1 Block diagram of single input multi output dc-dc Converter.

This study is mainly organized into five sections. Following the introduction, the converter design and analyses are given in Section II. In Section III, the design considerations of the proposed SIMO converter are discussed in detail. Section IV provides rich experimental results to validate the effectiveness of the proposed converter in practical applications. Finally, some conclusions are drawn in Section V.

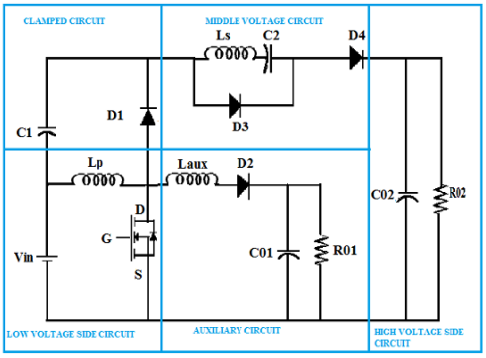

Fig. 2.SIMO Converter

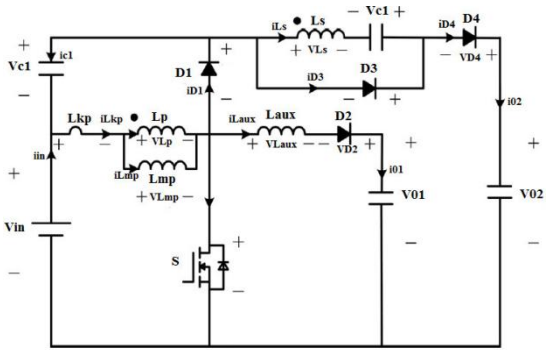

Fig. 3. Voltage polarities and CurrentDirection of SIMO Converter

The system configuration of the proposed high-efficiency SIMO converter topology to generate two different voltage levels from a

single-input power source is depicted in Fig. 2. This SIMO converter contains five parts including a low-voltage-side circuit (LVSC), a clamped circuit, a middle-voltage circuit, an auxiliary circuit, and a high-voltage-side circuit (HVSC). The major symbol representations are summarized as follows. V_{FC} (i_{FC}) and V_{O1} (i_{O1}) denote the voltages (currents) of the input power source and the output load at the LVSC and the auxiliary circuit, respectively; V_{O2} and i_{O2} are the output voltage and current in the HVSC. C_{FC}, C_{O1} , and C_{O2} are the filter capacitors at the LVSC, the auxiliary circuit, and the HVSC, respectively; C_1 and C_2 are the clamped and middle-voltage capacitors inthe clamped and middle-voltage circuits, respectively. L_P and L_S represent individual inductors in the primary and secondary sides of the coupled inductor T_r, respectively, where the primary side is connected to the input power source; L_{aux} is the auxiliary circuit inductor. The main switch is expressed as S_1 in the LVSC; the equivalent load in the auxiliary circuit is represented as R_{O1} , and the output load is represented as R_{O2} in the HVSC. The corresponding equivalent circuit given in Fig. 3 is used to define the voltage polarities and current directions. The coupled inductor in Fig.2 can be modeled as an ideal transformer including the magnetizing inductor L_{mp} and the leakage inductor L_{kp} in Fig. 3. The turns ratio N and coupling coefficient k of this ideal transformer are defined as

The turn's ratio (N) can be defined as

$$N=Ns/NP \quad (1)$$

The coupling coefficient is defined as

$$k=Lmp/(Lkp+Lmp) = Lmp/Lp \quad (2)$$

where $N1$ and $N2$ are the winding turns in the primary and secondary sides of the coupled inductor Tr. Because the voltage gain is less sensitive to the coupling coefficient and the clamped capacitor $C1$ is appropriately selected to completely absorb the leakage inductor energy , the coupling coefficient could be simply set at one (k = 1) to obtain Lmp= LP via (2). In this study, the following assumptions are made to simplify the converter analyses: 1) The main switch including its body diode is assumed to be an ideal switching element; and 2) The conduction voltage drops of the switch and diodes are neglected.

A. Operation Modes

The characteristic waveforms are depicted in Fig.5, and the topological modes in one switching cycle are illustrated in Fig. 4.

1) *Mode 1 (t_0 –t_1) [Fig. 4(a)]:* In this mode, the main switch S_1 was turned ON for a span, and the diode D_4 turned OFF. Because the polarity of the windings of the coupled inductor T_r is positive, the diode D_3 turns ON. The secondary current i_{Ls} reverses and charges to the middlevoltage capacitor C_2 . When the auxiliary inductor L_{aux} releases its stored energy completely, and the diode D_2 turns OFF, this mode ends.

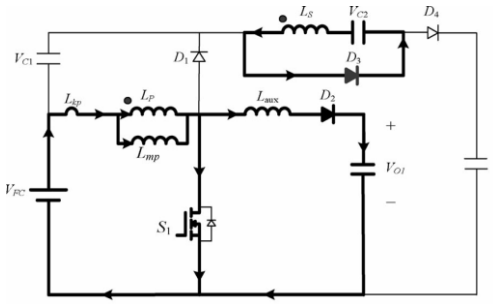

fig.4 (a)

2) *Mode 2 (t_1 –t_2) [Fig. 4(b)]:* At time $t = t_1$, the main switch S_1 is persistently turned ON. Because the primary inductor L_P is charged by the input power source, the magnetizing current i_{Lmp} increases gradually in an approximately linear way. At the same time, the secondary voltage v_{Ls} charges the middle-voltage capacitor C_2 through the diode D_3. Although the voltage v_{Lmp} is equal to the input voltage V_{FC} both at modes 1 and 2, the ascendant slope of the leakage current of the coupled inductor (di_{Lkp}/dt) at modes 1 and 2 is different due to the path of the auxiliary cicuit. Because the auxiliary inductor L_{aux} releases its stored energy completely, and the diode D_2 turns OFF at the end of mode 1, it results in the reduction of di_{Lkp}/dtat mode 2.

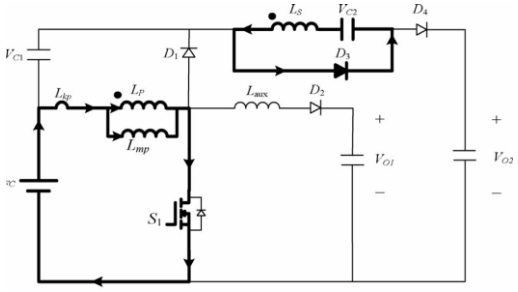

fig.4 (b)

3) *Mode 3 (t_2 –t_3) [Fig. 4(c)]:* At time t = t_2 , the main switch S_1 is turned OFF. When

the leakage energy still released from the secondary side of the coupled inductor, the diode D_3 persistently conducts and releases the leakage energy to the middle-voltage capacitor C_2 . When the voltage across the main switch v_{S1} is higher than the voltage across the clamped capacitor V_{C1} , the diode D_1 conducts to transmit the energy of the primary-side leakage inductor L_{kp} into the clamped capacitor C_1 . At the same time, partial energy of the primary-side leakage inductor L_{kp} is transmitted to the auxiliary inductor L_{aux}, and the diode D_2 conducts. Thus, the current i_{Laux} passes through the diode D_2 to supply the power for the output load in the auxiliary circuit. When the secondary side of the coupled inductor releases its leakage energy completely, and thediode D_3 turns OFF, this mode ends.

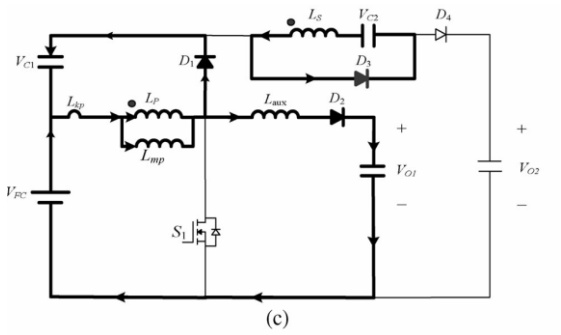

fig.4 (c)

4) ***Mode 4 (t3 –t4) [Fig. 4(d)]:*** At time $t = t3$, the main switch $S1$ is persistently turned OFF. When the leakage energy has released from the primary side of the coupled inductor, the secondary current *iLS* is induced in reverse from the energy of the magnetizing inductor *Lmp* through the ideal transformer, and flows through the diode $D4$ to the HVSC. At the same time, partial energy of the primary side leakage inductor *Lkp* is still persistently transmitted to the auxiliary inductor *L*aux, and the diode $D2$ keeps to conduct. Moreover, the current *iL*aux passes through the diode $D2$ to supply the power for the output load in the auxiliary circuit.

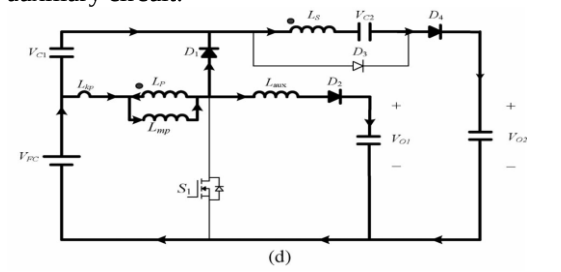

fig.4 (d)

5) ***Mode 5 (t4 –t5) [Fig. 4(e)]:*** At time $t = t4$, the main switch $S1$ is persistently turned OFF, and the clamped diode $D1$ turns OFF because the primary leakage current *iLkp* equals to the auxiliary inductor current *iL*aux. In this mode, the input power source, the primary winding of the coupled inductor *Tr*, and the auxiliary inductor *L*aux connect in series to supply the power for the output load in the auxiliary circuit through the diode $D2$. At the same time, the input power source, the secondary winding of the coupled inductor *Tr*, the clamped capacitor $C1$, and the middlevoltage capacitor ($C2$) connect in series to release the energy into the HVSC through the diode $D4$.

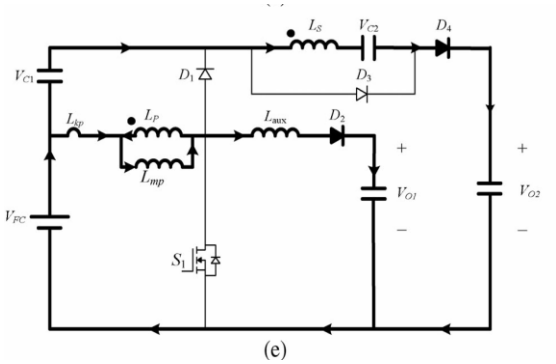

fig.4 (e)

6) ***Mode 6 (t5 –t6) [Fig. 4(f)]:*** At time $t=t5$, this mode begins when the main switch $S1$ is triggered. The auxiliary inductor current *iL*aux needs time to decay to zero, the diode $D2$ persistently conducts. In this mode, the input power source, the clamped capacitor $C1$, the secondary winding of the coupled inductor *Tr*, and the middle-voltage capacitor $C2$ still connect in series to release the energy into the HVSC through the diode$D4$. Since the clamped diode$D1$ can be selected as a low-voltage Schottky diode, it will be cut off promptly without a reverse-recovery current. Moreover, the rising rate of the primary current *iLkp* is limited by the primary-side leakage inductor *Lkp*. Thus, one cannot derive any currents from the paths of the HVSC, the middle-voltage circuit, the auxiliary circuit, and the clamped circuit. As a result, the main switch $S1$ is turned ON under the condition of ZCS and this soft-switching property is helpful for alleviating the switching loss. When the secondary current *iLS* decays to zero, this mode ends. After that, it begins the next switching cycle and repeats the operation in mode 1.

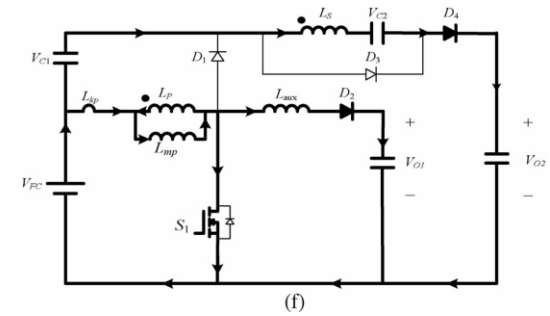

fig.4(f)

B. Characteristic waveforms of SIMO converter :

The characteristic waveform of SIMO convertor is shown in fig.5. The switching period is denoted as T_s. The switching period is divided into six modes. The different operational modes of the converter are explained in above section.

The ON period can be written in terms of duty cycle d_1 as

$T_{ON} = d_1.T_s$

The OFF period can be written as

$T_{OFF} = (1-d_1)\ T_s$

Voltage and current waveforms through all the devices in the circuit are plotted in fig.5. The nature of these waveforms and operational modes of the converter are taken into consideration while deriving the design equations of the converter.

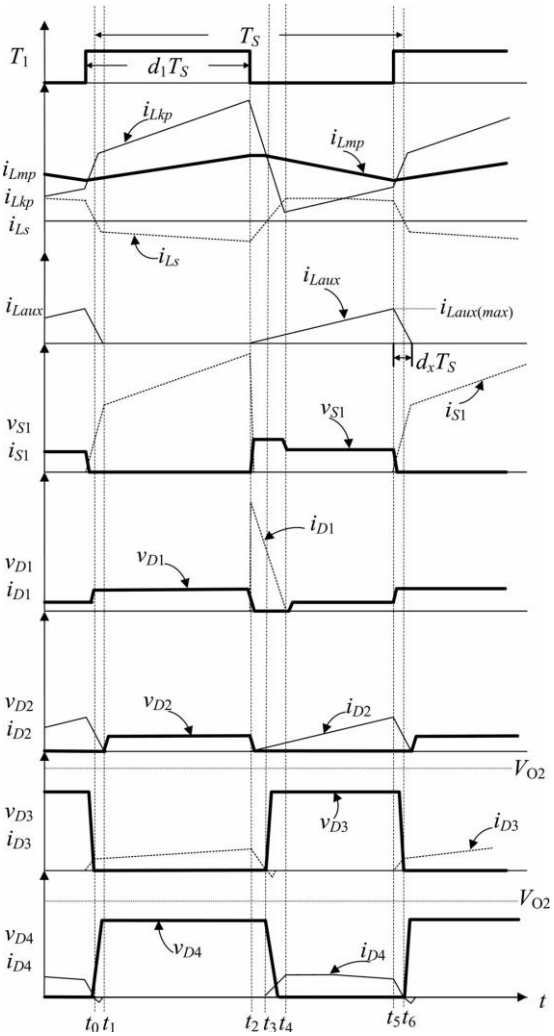

Fig.5 Characteristic waveforms of high-efficiency SIMO converter.

Remark 1:In general, a dc–dc converter operated at the continuous conduction mode (CCM) can provide a low ripple current for protecting the energy source. In the proposed SIMO converter, it is operated at the CCM due to the design of the auxiliary inductor. The coupled inductor is charged by the input power source when the main switch is turned ON, and the coupled inductor releases its energy to the auxiliary inductor when the main switch is turned OFF until the energy balance of the coupled inductor and the auxiliary inductor is established

C. Voltage Gain Derivation

Since the magnetizing inductor voltage v_{Lmp} is equal to the input power source V_{FC} at the mode 2, the voltage v_{Lmp} can be represented as

$$v_{Lmp}=V_{FC}. \quad (3)$$

Due to the relation of $v_{Ls}=Nv_{Lp}=V_{C2}$, the voltage V_{C2} can be represented as

$$V_{C2} = NV_{FC}. \quad (4)$$

By using the voltage-second balance , the relation of the average voltage across the magnetizing inductor L_{mp} of the coupled inductor T_r to be zero can be represented as

$$V_{FC}d_1T_S + v_{Lmp}(1 - d_1)T_S = 0 \quad . (5)$$

From (5), one can obtain

$$v_{Lmp}= [-d_1/(1 - d_1)]V_{FC}. \quad (6)$$

Since the voltage of the clamped capacitor V_{C1} is equal to the negative voltage of magnetizing inductors voltage v_{Lmp} at modes 3 and 4, the voltage V_{C1} can be expressed via (6) as

$$V_{C1} = -v_{Lmp}= [d_1/(1 - d_1)]V_{FC} \quad (7)$$

According to Kirchhoff's voltage law, the output voltage V_{O2}can be obtained as

$$V_{O2} = V_{FC} + V_{C1} + V_{C2} - v_{Ls}. \quad (8)$$

By using the voltage-second balance , the relation of the average voltage across the secondary winding $v_{Ls}$to be zero can be expressed by (4) and (8) as

$$(NV_{FC})d_1T_S+(V_{FC}+V_{C1}+V_{C2}-V_{O2})(1-d_1)T_S = 0 \quad (9)$$

From (4)–(9), the voltage gain G_{VH} of the proposed SIMO converter from the LVSC to the HVSC can be given as

$$G_{VH}=\frac{V02}{VFC}=\frac{N+1}{1-d1} \quad (10)$$

For calculating the discharge time of the auxiliary inductor at modes 1 and 6, the corresponding time interval can be denoted as $d_xT_s= [(t_6 - t_5) + (t_1 - t_0)]$. By using the voltage-second balance , the relation of the average voltage across the auxiliary inductor $L_{aux}$to be zero can be represented as

$$(V_{FC} - v_{Lmp} - V_{O1})(1 - d_1)T_S + (-V_{O1})d_xT_S = 0 \quad (11)$$

The voltage gain G_{VL} of the proposed SIMO converter from the LVSC to the auxiliary circuit can be obtained by (6) and (11) as

$$G_{VL}=\frac{V01}{VFC}=\frac{1}{1-d1-dx} \quad (12)$$

Because the diode current i_{D2} is equal to the current i_{Laux}, the average value of the diode current i_{D2} can be calculated from the third graph in Fig. 3 as

$$I_{D2(AVG)}=\frac{1}{Ts}\left[\frac{1}{2}iLaux(max)(1-d1)Ts + \frac{1}{2}iLaux(max)dxTs\right] \quad (13)$$

Where T_S is the converter switching cycle, $i_{Laux(max)}$ is the maximum current of the auxiliary inductor and can be expressed as

$$iLaux(max)=\left(\frac{V01}{Laux}\right)dx\,Ts \quad (14)$$

By substituting (14) into (13), one can obtain

$$i_{D2(AVG)}=\frac{V01}{2Laux}dxTs(1-d1+dx) \quad (15)$$

Because the average current of the diode D_2 is equal to the current i_{O1}, it yields

$$i_{D2(AVG)}=\frac{V01}{R01} \quad (16)$$

From (15) and (16), the duty cycle d_x can be rewritten as

$$d_x=\frac{-(1-d1)+\sqrt{(1-d1)2+[8Laux/(R01\,Ts)]}}{2} \quad (17)$$

By substituting (17) into (12), the voltage gain G_{VL} of the proposed SIMO converter from the LVSC to the auxiliary circuit can be rearranged as

$$G_{VL}=\frac{V01}{VFC}=\frac{2}{(1-d1)+\sqrt{(1-d1)2+[8Laux/(R01\,Ts)]}} \quad (18)$$

III. Design Considerations

In a FC generation system, except for the FC stack itself, some other auxiliary components, such as the BOP including an electronic control board, an air compressor, and a cooling fan, are required. To verify the effectiveness of the proposed SIMO converter topology, a 12-V power supply V_{FC} is taken as the input source to imitate a FC stack, and a 24-V battery module is utilized for the output load in the auxiliary circuit. Moreover, the maximum battery floating charge voltage is set at 28 V, and the allowable charging power is 100 W (R_{O1} = 7.84 Ω). In addition, the desired output voltage V_{O2} is set at 200 V in the HVSC, and the maximum output power in the HVSC is 1.1 kW (R_{O2} = 36.36 Ω). Define the minimum and maximum output powers in the auxiliary circuit and the HVSC as ($P_{1\,min}$, $P_{1\,max}$) and ($P_{2\,min}$, $P_{2\,max}$), respectively. In the case of resistive loads, one can, respectively, obtain the minimum and maximum resistances connected at the auxiliary circuit and the HVSC as ($R_{O1\,min} = G_{2VL}V_{2FC}/P_{1\,max}$, $R_{O1\,max} = G_{2VL}V_{2FC}/P_{1\,min}$) and ($R_{O2\,min} = G_{2VH}V_{2FC}/P_{2\,max}$, $R_{O2\,max} = G_{2VH}V_{2FC}/P_{2\,min}$) according to (10) and (12). Furthermore, this converter is operated with a 100-kHz switching frequency (f_S= 100 kHz), and the coupling coefficient could be simply set at one (k = 1) because the proposed circuit has a good clamped effect. By substituting N = 1– 7 into (10), the curve of the voltage gain G_{VH} with respect to different duty cycles d_1 is depicted in Fig. 5. Moreover, the curve of the voltage gain G_{VL} with respect to different duty cycles d_1 can be represented as Fig. 6 by substituting L_{aux}= 1– 7μH, T_S = 10 μs, and $R_{O\,1}$ = 7.84 Ω into (18). By analyzing Fig. 5, the turns ratio of the coupled inductor can be selected as N = 5 when the operational conditions are V_{O2} = 200V and V_{FC} = 12V (i.e., G_{VH} = 16.67), so that the corresponding duty cycle can be obtained as d_1 = 0.64. This value is reasonable in practical applications. As can be seen from Fig. 3, the relation of $d_x < d_1$ should be satisfied. According to (17), the limit for L_{aux} can be calculated as $L_{aux}<0.5d_1R_{O1}T_S$. By considering V_{FC} = 12V, V_{O1} = 28 V, and d_1 = 0.64, the value of the auxiliary inductor can be obtained as L_{aux}= 2 μH from Fig. 6.

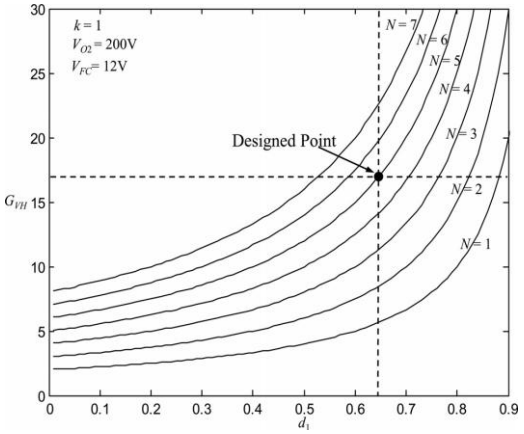

Fig.6. Voltage gain G_{VH} with respect to duty cycle d_1 under different turns ratios.

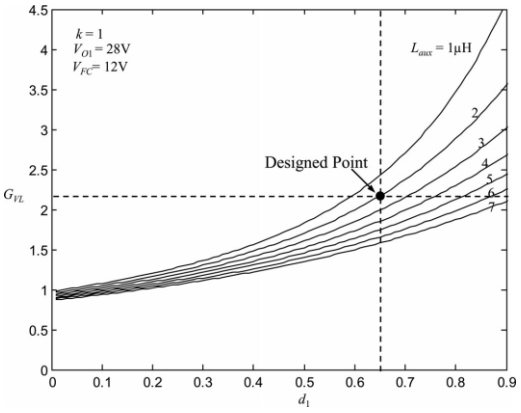

Fig. 7. Voltage gain G_{VL} with respect to duty cycle d_1 under different auxiliary inductor values

Because the voltage across the main switch S_1 at the mode 3 can be represented as

$v_{S1} = V_{C1} + V_{FC} = [1/(1-d_1)]V_{FC}$,

and the voltage relation between the LVSC and the HVSC according to (10) can be given by

$V_{FC} = [(1-d_1)/(N+1)]V_{O2}$,

the voltage across the main switch S_1 can be rewritten as

$$v_{S1} = \frac{V02}{(N+1)} \qquad .(19)$$

By analyzing (19), the switch voltage v_{S1} is not related to the input power source V_{FC} and the duty cycle d_1 if the values of the output voltage V_{O2} and the turns ratio N are fixed. Thus, the switch voltage v_{S1} can be clamped at 33.3 V by substituting N = 5 and V_{O2} = 200V into (19). As long as the input voltagein the LVSC is not higher than the output voltage in the HVSC, the proposed SIMO converter can be applied well to the input power source with voltage variations. To consider the ring phenomena
caused by the circuit stray inductance and the parasitic capacitance of the main switch S_1 , the main switch S_1 with a 75-V voltage rating is selected in the proposed SIMO converter. In this study, the clamped diode D_1 should be a fast conductive device. Because the clamped voltage of the diode D_1 is the same as the one of the main switch S_1 , a low-voltage Schottky diode can be adopted to conduct promptly with lower conduction loss and reverse-recovery current. During the mode 2, the diode D_2 turns OFF, and its voltage can be represented by

$v_{D2} = V_{O1} + [L_{aux}(di_{D2}/dt)]$.

Since the ascendant slope of the diode current (di_{D2}/dt) is equal to zero at the mode 2, the voltage v_{D2} can be rearranged as $v_{D2} = V_{O1}$. According to V_{O1} = 28 V, the voltage stress on the diode D_2 is smaller than 100 V. Thus, a low-voltage Schottky diode also can be selected to reduce the conduction loss and the reverserecovery current. The voltage across the diodes D_3 and D_4 , which can be expressed by

$v_{D3,D4} = V_{O2} - (V_{C1} + V_{FC}) = [N/(N + 1)]V_{O2}$, is 166.67V by considering N = 5 and V_{O2} = 200V. Thus, the diodes (D_3 andD_4) with 200 V voltage ratings can be selected. When the main switch S_1 is turned ON during modes 1, 2, and 6, the voltage across the magnetizing inductor is $v_{Lmp} = V_{FC}$ = 12V. Moreover, the relation between the current and voltage of the magnetizing inductor can be represented as $v_{Lmp} = L_P(di/dt)$. If the current range di is designed as 30 A and $dt = d_1T_S$ = 6.4 μs, one can calculate the value of L_P as 2.56 μH. In order to manufacture the couple inductor easily, the number of winding turns in the primary side of the coupled inductor is N_1 = 2, and its measured inductor value is L_P = 3 μH. Because the ratio of the primary and secondary inductors in the coupled inductor is square proportional to the turns ratio (N = 5), the value of L_S can be determined as 75 μH, and the winding turns in the secondary side of the coupled inductor is N_2 = 10 in this study.

In this study, an EE-55 core with the magnetic flux density 390 mT, the maximum magnetic flux 138 μWb, the cross section area 354 mm^2 ,and the designed air gap 1.5 mm is adopted as the magnetic core of the coupled inductor. According to the magnetic circuit law, the air resistance can be calculated as 3.4 MΩ. By considering the maximum output power 1.1 kW with the corresponding conversion efficiency 85%, the maximum input current is about 107.84 A, and the maximum magnetizing current is about 122.84 A. The produced magnetic flux can be obtained as 72.25 μWb by using the primary winding turns (N_1 = 2), maximum magnetizing current (122.84 A), and air resistance (3.4MΩ). Thus, the saturation phenomenon of the magnetizing current can be prevented by the designed magnetic core of the coupled inductor. In the proposed SIMO converter, the electric charge variation ΔQ_1 of the filter capacitor for the auxiliary circuit can be represented as $\Delta Q_1 = (V_{O1}/R_{O1})(d_1 - d_x)T_S = C_{O1}\Delta V_{O1}$, and the voltage ripple of V_{O1} can be rearranged as $(\Delta V_{O1}/V_{O1}) = (d_1 - d_x)/(R_{O1}C_{O1}f_S)$. By substituting d_1 = 0.64, R_{O1} =7.84 Ω, T_S = 10 μs, and L_{aux}= 2 μH into (17), the duty cycle d_x can be calculated as 0.11. If one sets the voltage ripple of V_{O1} to be less than 1%, the value of C_{O1} should be selected over 67.6 μF by substituting d_1 = 0.64, d_x = 0.11, R_{O1} = 7.84 Ω, f_S= 100 kHz, and V_{O1} = 28 V into the function of $C_{O1} = (d_1 - d_x)/[(R_{O1}f_S)(\Delta V_{O1}/V_{O1})]$. Moreover, the electric charge variation of the filter capacitor $\Delta Q_2$for the HVSC can be expressed as $\Delta Q_2 = (V_{O2}/R_{O2})d_1T_S = C_{O2}\Delta V_{O2}$, and the ripple of the

output voltage V_{O2} can be rearranged as $(\Delta V_{O2}/V_{O2}) = d_1/(R_{O2}C_{O2}f_S)$. By substituting f_S= 100 kHz, d_1 = 0.64, R_{O2} = 36.36 Ω, and V_{O2} = 200V into the function of $C_{O2} = d_1/[(R_{O2}f_S)(\Delta V_{O2}/V_{O2})]$, the value of C_{O2} should be chosen over 17.6 μF with the constraint on the output voltage ripple to be less than 1%. According to the previous consideration, the values of C_{O1} = 100 μF and C_{O2} = 20 μF are adopted in the experimental prototype. Due to a high switching frequency (f_S= 100 kHz) in the proposed SIMO converter, the factors of lower equivalent series resistance and faster dynamic response should be considered in the design of the clamped capacitor C_1 and the middle-voltage capacitor C_2 for reducing the capacitor voltage ripples. In this study, metalized-polyester film capacitors are adopted for $C_1$and C_2 for satisfying the fast charge and discharge property. In order to further minimize the current and voltage ripples imposed to the main switch S_1 and the diodes D_3 and D_4, the cutoff frequencies of the $L_P - C_1$ and $L_S - C_2$ filters are taken to be at least ten times smaller than the switching frequency. According to the previous consideration, the values of C_1 and C_2 are, respectively, chosen as 85 and 10 μF in the proposed SIMO converter so that the corresponding resonant frequencies are

$f_{01} \equiv 1/(2\pi\sqrt{LpC1}$ =9.97kHz and

$f_{02} \equiv 1/(2\pi\sqrt{LsC2})$=5.81 kHz.

In this study, the dc voltage feedback control is used to solve the problem of the output voltage of the HVSC varied with load variations, and a digital-signal-processor TMS320F2812 manufactured by Texas Instruments is adopted to achieve this goal of feedback control. In this feedback scheme, conventional PWM control without detailed mathematical dynamic model is utilized, and its formula can be represented as $V_{com1} = k_p V_{err} + k_i \int_0^t V_{err} dt$, where kp and k_i are proportional and integral gains, respectively; $V_{err} = V_{cmd} - V_{O2}$ is the voltage tracking error, in which V_{cmd} is the voltage command. The value of k_p= 5 is designed according to the amount of initial tracking error, and the value of k_i= 0.05 is selected based on the amount of steady-state error. The driving signal T_1 is generated by comparing the control signal V_{com1} with the carrier wave v_{tri1} .

IV. Experimental Results

The fig.8 shows the simulation block diagram of the SIMO converter with one input source and two outputs having common ground. The only switch in the converter is controlled using PWM Controller. The output of the high voltage side circuit can be effectively controlled using the duty cycle ‘d1’ of the switch. The output of the low voltage side circuit can be controlled by changing the value of auxiliary inductor and hence the duty cycle ‘dx’ of the auxiliary inductor.

The values of various elements used for simulation are:

Input voltage source Vin = 12 V

Clamped Capacitor C1 = 85μF

Middle voltage capacitor C2 = 10 μF

Filter capacitor C01=100 μF

Filter Capacitor C02=200 μF

Load Resistance of HVSC R02 =200

Load Resistance of LVSC R01 =10

Auxiliary inductor Laux = 2μH

Primary of Coupled Inductor Lp = 3μH

Secondary of Coupled Inductor Ls =75μH

A. Simulation Diagrame

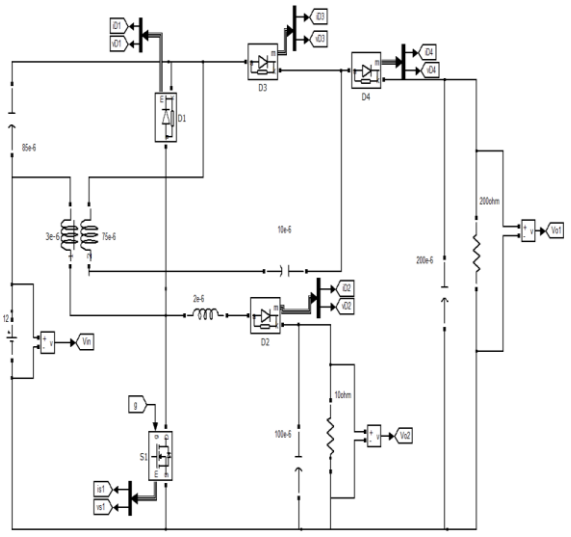

fig.8. Simulation diagram for SIMO converter

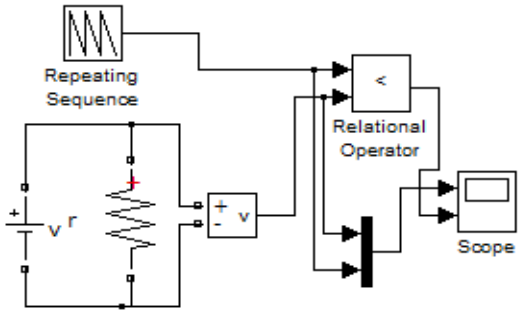

fig.9. Simulation diagram for PWM block

B. Simulation Results

HVSC output voltage = 200V
Auxiliary side output voltage = 26.5V
Fig. 10 shows the input voltage waveform, output waveforms of HVSC side and auxiliaryside.

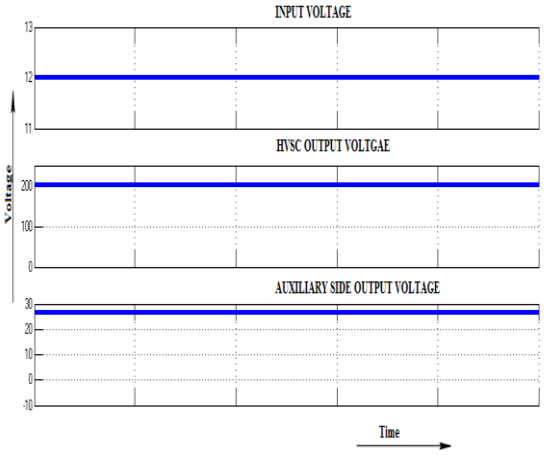

Fig. 10. Input and output voltage waveforms of SIMO Converter

The voltage and current waveform of the switch indicating soft switching is given in fig. 11

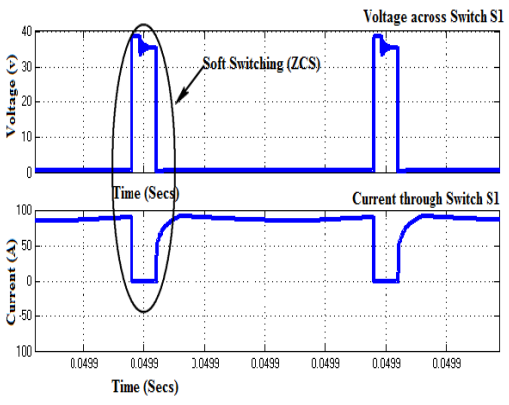

Fig. 11. Voltage and current waveform of the Switch

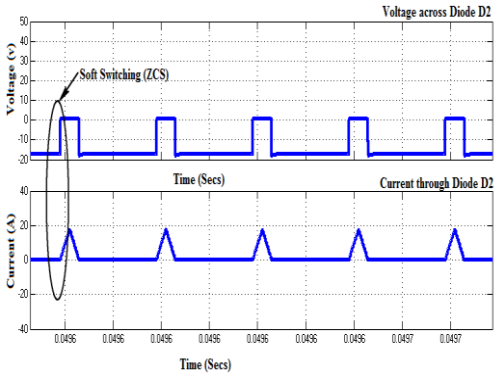

Fig. 12. Voltage and current in diode D2

Fig. 13. Shows the voltage across and current through the diode D2 which is in series with auxiliary inductor. It is clear from the fig. 12 that switching of diode D2 is at ZCS condition.

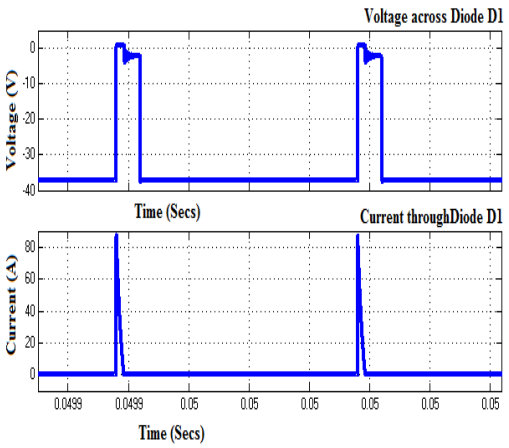

Fig. 13. Voltage and Current through Diode D1

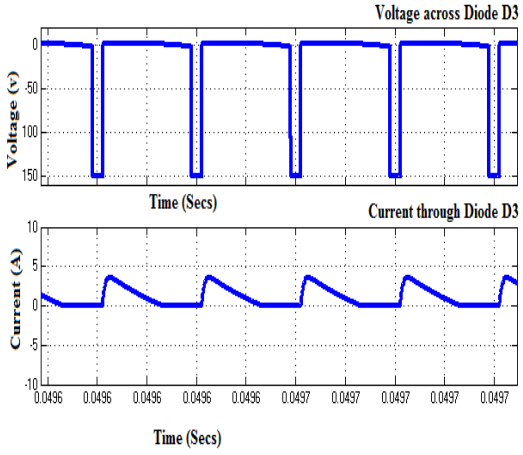

Fig. 14 Voltage and Current through Diode D_3

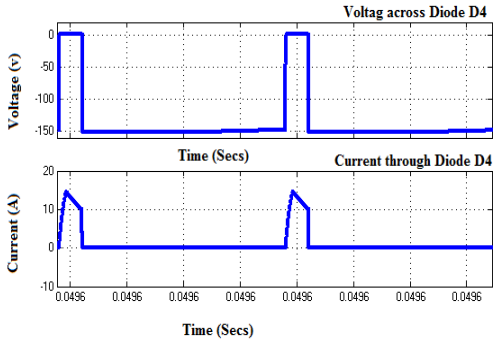

Fig. 15 Voltage and Current through Diode D_4

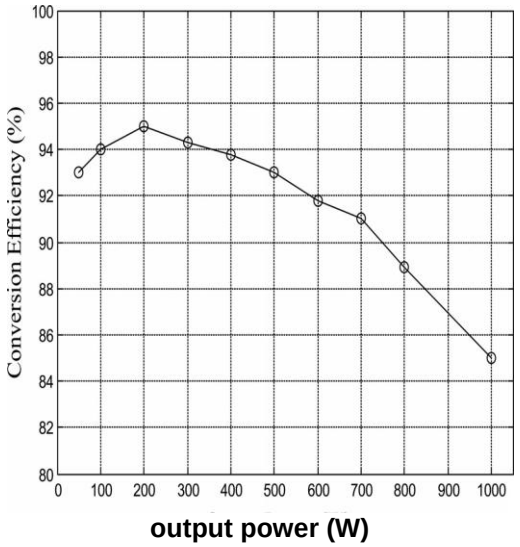

Fig. 16. Conversion efficiency of SIMO converter for V_{FC} = 12 V, V_{O1} = 24–28 V, and V_{O2} = 200 V under different powers.

V. CONCLUSION

This study has successfully developed a high-efficiency SIMO dc–dc converter, and this coupled-inductor-based converter was applied well to a single-input power source plus two output terminals composed of an auxiliary battery module and a high-voltage dc bus. The experimental results reveal that the maximum efficiency was measured to exceed 95%, and the average conversion efficiency was measured over 91%. The proposed SIMO converter is suitable for the application required one common ground, which is preferred in most applications. However, it is not appropriate to be used as the active front for dc–ac multilevel inverters. This limitation is worthy to be investigated in the future research.

The major scientific contributions of the proposed SIMO converter recited as follows:

1) This topology adopts only one power switch to achieve the objective of high-efficiency SIMO power conversion

2) The voltage gain can be substantially increased by using a coupled inductor

3) The stray energy can be recycled by a clamped capacitor into the auxiliary battery module or high-voltage dc bus to ensure the property of voltage clamping

4) An auxiliary inductor is designed for providing the charge power to the auxiliary battery module and assisting the switch turned ON under the condition of ZCS

5) The switch voltage stress is not related to the input voltage so that it is more suitable for a dc power conversion mechanism with different input voltage levels

6) The copper loss in the magnetic core can be greatly reduced as a full copper film with lower turns. This high-efficiency SIMO converter topology provides designers with an alternative choice for boosting a low-voltage power source to multiple outputs with different voltage levels efficiently. The auxiliary battery module used in this study also can be extended easily to other dc loads, even for different voltage demands, via the manipulation of circuit components design.

REFERENCES

[1] Chen.Y and Kang.Y;"A full regulated dual-output dc-dcconverter with special-connected two transformers(SCTTs) cell and complementary pulse widthmodulation-PFM(CPWM-PFM)," IEEE Trans. PowerElectron., vol. 25, no. 5, pp. 1296–1309, May 2010

[2] Chen.Y, Kang.Y, Nie.S, and Pei.X; "The multiple-outputDC–DC converter with shared ZCS lagging leg," IEEETrans. Power Electron., vol. 26, no. 8, pp. 2278–2294,Aug. 2011.

[3] Ellis M.W,.VonSpakovsky M.R, and Nelson D.J;"Fuelcell systems: Efficient, flexible energy conversion for the21 st century,"Proc. IEEE, vol. 89, no. 12, pp. 1808– 1818, Dec. 2001

[4]GaminiJayasinghe.S.D,MahindaVilathgamuwa.D , andMadawalaU.K,;"Diode-clamped three-level inverterbasedbat-tery/supercapacitordirect integration schemefor renewable energy sys-tems," IEEE Trans. PowerElectron., vol. 26, no. 6, pp. 3720–3729, Dec. 2011.

[5] Kim.T, Vodyakho.O, and Yang.J; "Fuel cell hybridelectronic scooter,"IEEE Ind. Appl. Mag., vol. 17, no. 2,pp. 25–31, Mar./Apr. 2011.

[6] Gao.F, Blunier.B, Sim.M.G˜ oes, and Miraoui.A; "PEMfuel cell stack modeling for real-time emulation inhardware-in-the-loop application,"IEEE Trans. EnergyConvers., vol. 26, no. 1, pp. 184–194, Mar. 2011

[7] Kirubakaran.A, Jain., and NemaR.K; "DSP-controlledpower elec-tronic interface for fuel-cell-based distributedgeneration," IEEE Trans. Power Electron., vol. 26, no.12, pp. 3853–3864, Dec. 2011.

[8] Kim.J.K, Choi.S.W, and Moon.G.W; "Zero-voltageswitching post regulation scheme for multi outputforward converter with synchronous switches," IEEETrans. Ind. Electron., vol. 58, no. 6, pp. 2378–2386,Jun.2011

[9] Liu.B, Duan.S, and Cai.T,; "Photovoltaic dc-buildingmodule-based BIPV system-concept and designconsiderations," IEEE Trans. Power Electron., vol. 26,no. 5, pp. 1418–1429, May 2011.

[10] Mohan.N, UndelandT.M, and Robbins.W.P; PowerElectronics: Con-verters, Applications, and Design. NewYork: Wiley, 1995.

[11] Nami.A, Zare.F, Ghosh.A, and Blaabjerg.F; "MultipleoutputDC–DC converters based on diode-clampedconverters configuration: Topology and control strategy,"IET Power Electron., vol. 3, no. 2, pp. 197–208, 2010.

[12] Pan.C.T, Cheng.M.C, and Lai.C.M; "A novel integrateddc/ac converter with high voltage gain capability fordistributed energy resource systems," IEEE Trans. PowerElectron., vol. 27, no. 5, pp. 2385–2395, May 2012

[13] Patra.P, Patra.A, and Misra.A;"A single-inductormultiple-output switcher with simultaneous buck, boostand inverted outputs," IEEE Trans. Power Electron., vol.27, no. 4, pp. 1936–1951, Apr. 2012